



## Investigation of crack paths in natural fibre-reinforced composites

S. Keck, M. Fulland

*University of Applied Sciences Zittau/Görlitz, Germany*

*s.keck@hszg.de, m.fulland@hszg.de*

---

**ABSTRACT.** Nowadays, fibre-reinforced composite materials are widely used in many fields, e.g. automotive and aerospace. Natural fibres such as flax and hemp provide good density specific mechanical properties. Additionally, the embodied production energy in natural fibres is much smaller than in synthetic ones. Within this paper the fracture mechanical behaviour of flax fibre-reinforced composites is discussed. Especially, this paper focuses on the determination and investigation of crack paths in compact tension specimens with three different fibre directions under a static as well as fatigue load. Differences and similarities in the obtained crack paths under different loading conditions are presented. Due to the pronounced orthotropic behaviour of those materials the crack path is not only governed by the stress state, but practically determined by the fibre direction and fibre volume fraction. Therefore, the well-known stress intensity factor solutions for the standard specimens are not applicable. It is necessary to carry out extensive numerical simulations to evaluate the stress intensity factor evolution along the growing crack in order to be able to determine fatigue crack growth rate curves. Those numerical crack growth simulations are performed with the three-dimensional crack simulation program ADAPCRACK3D to gain energy release rates and in addition stress intensity factors.

**KEYWORDS.** Natural fibre-reinforced composites; Orthotropic material behaviour; Crack paths; Fatigue crack growth rate curves; ADAPCRACK3D.

---

### INTRODUCTION

Due to their mechanical properties (stiffness and strength) and their small densities fibre-reinforced composite materials are widely used in many fields such as automotive and aerospace. Hence, their utilisation for lightweight applications is suitable. Furthermore, it is of great importance to take renewable resources into account which are comparable in terms of mechanical properties with conventional materials. Concerning this matter natural fibres need to be considered. The embodied production energy in natural fibres is in the order of 10 times smaller than in synthetic ones. Additionally, the production of greenhouse gases is enormously reduced [1]. Within this paper the fracture mechanical behaviour of natural fibre-reinforced composites is discussed. In this work composites are defined as petrochemical polymers reinforced with flax-fibres. The fibres take up forces. The matrix transfers forces to fibres, fixes, and protects those from surrounding conditions. The ratio of fibre volume and composite volume defines the fibre volume fraction. Thereby, tailored construction components and structures can be built. Due to the pronounced orthotropic behaviour of those materials the crack path is not only governed by the stress state, but practically determined by the fibre direction and the fibre volume fraction.

---

At first, materials and specimens are explained. Then experimental investigations and numerical computations are described. Later on the identified crack paths and fatigue crack growth curves are illustrated. Finally, conclusions of the obtained results and an outlook are given.

## MATERIAL AND SPECIMENS

In this work the composite is reinforced with flax-fibres, which are semi-finished products (yarn and twisted yarn). Their density is about  $1,450 \text{ kg/m}^3$  [1]. For the polymer matrix an epoxy resin is used. The fibres get rolled on a frame to achieve a unidirectional alignment (Fig. 1). Due to the orthotropic behaviour of the fibres and the unidirectional alignment the composites are orthotropic, too.

Unnotched specimens and compact tension specimens were taken from plates (geometric dimensions:  $500 \text{ mm} \times 470 \text{ mm} \times 10 \text{ mm}$ ). The size of an unnotched specimen is  $150 \text{ mm} \times 15 \text{ mm} \times 10 \text{ mm}$ . The geometric dimensions of the compact tension specimens (Fig. 2) are chosen according to the ASTM standard E647-13 [2]. Due to the smaller mechanical properties (Fig. 3) compared to metallic materials the drill holes are reduced. The specimen depth is set to  $10 \text{ mm}$ . A post-curing process provides a higher strength of the polymer matrix. For each compact tension specimen the pre-crack initiation is produced with a razor blade (razor sawing).



Figure 1: Semi-finished product consisting of flax.

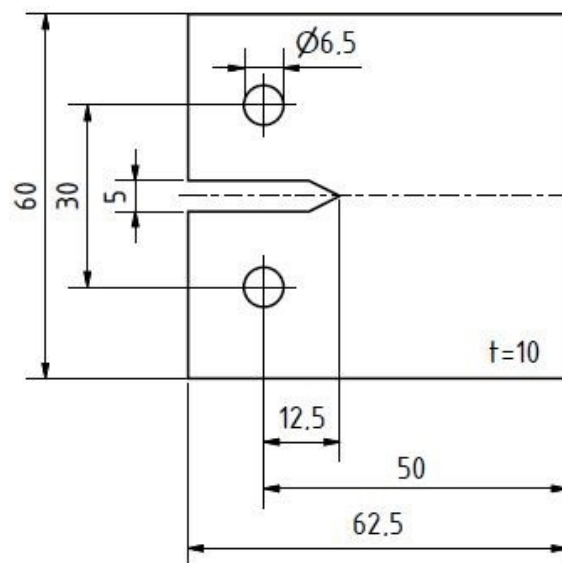


Figure 2: Geometric dimensions of the investigated compact tension specimen (dimensions in mm).

## EXPERIMENTAL INVESTIGATIONS

### *Mechanical properties*

The Young's moduli are measured by a universal testing machine (Zwick Roell Z250) under ambient temperature. Tensile tests were conducted to characterize the mechanical properties, which are required to execute the numerical simulations with real values. The mean values and the standard deviations of the Young's moduli of the unnotched specimens with different fibre directions and fibre volume fractions are plotted in Fig. 3. Thereby, character 'F' stands for flax. The number left to the slash describes the yarn count (unit: meters per gram). A '1' behind the slash marks a yarn and a '2' would mean a twisted yarn. Subsequently, fibre volume fraction and fibre direction are named. The fibre directions are illustrated schematically in Fig. 4.

Both constituents (fibres and polymer matrices) and composites have brittle fracture behaviour. Additionally, tensile test results show that there is a non-linear behaviour of the composites.

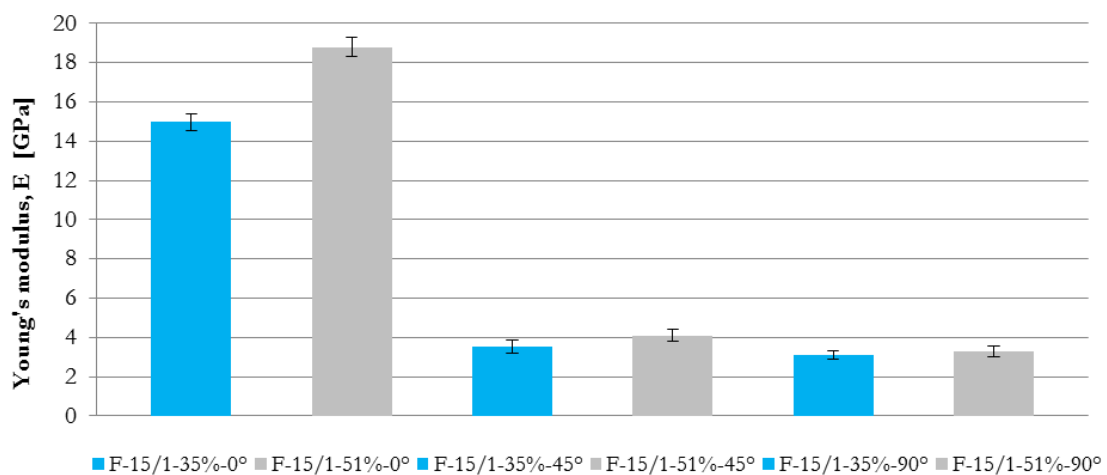


Figure 3: Young's moduli of unnotched specimens.

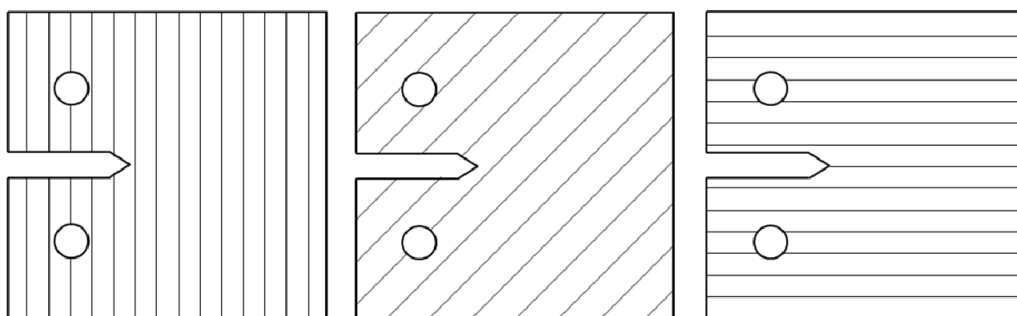


Figure 4: Schematic illustration of compact tension specimens with different fibre directions (0°, 45°, 90°).

### *Crack paths*

The crack paths of the compact tension specimens were determined under static as well as cyclic loading conditions. In fatigue tests the stress ratio  $R$  is set to 0.1. Different values of remote tensile forces were applied, thus, the initial crack is in Mode I. Fig. 5 shows the crack paths of the specimens (fibre volume fraction 35%) under constant amplitude cyclic loading. After executing fatigue tests those were loaded until failure. If the fibre direction is perpendicular to the loading direction, the fatigue crack grows along the fibres (Fig. 5, right hand side). This particular crack path is identical with a path in homogeneous isotropic materials. If the angle between fibre direction and loading direction is about 45°, the crack path kinks at the crack tip and grows along the fibre direction (Fig. 5, middle). If the reinforced direction is parallel to the loading direction, the fatigue crack kinks at the crack tip in fibre direction and grows along the fibres (Fig. 5, left hand

side). In either case the crack paths are determined by the fibre direction and there are inter-fibre failures. The same crack paths were obtained by testing compact tension specimens under static loading.

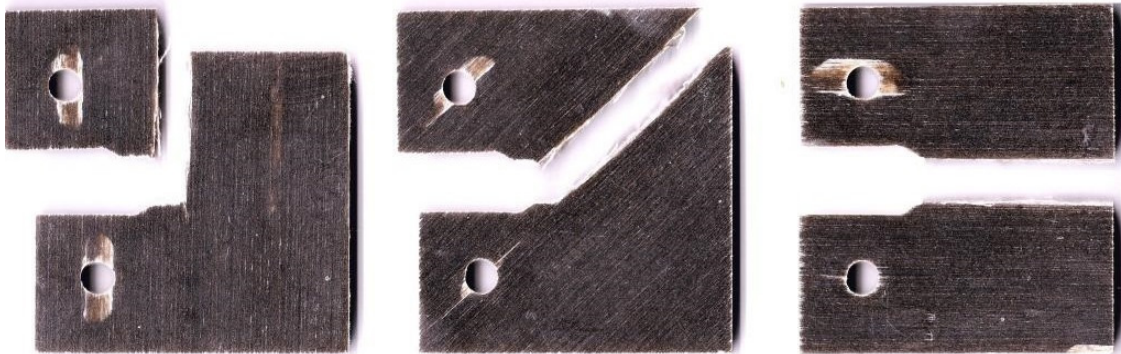


Figure 5: Compact tension specimens with different directions after cyclic loading (fibre volume fraction 35%).

Further investigations showed that there is a relation between fibre volume fractions and crack paths. The dependence on the fibre volume fraction using compact tension specimens (0° fibre direction, constant amplitude cyclic loading,  $R = 0.1$ ) is illustrated in Fig. 6. The more fibres are contained, the faster the crack path tends to grow in fibre direction.



Figure 6: Compact tension specimens with different fibre volume fractions (0° fibre direction).

### FATIGUE CRACK GROWTH RATE CURVES

The fatigue tests were conducted on a resonance testing machine (Roell Amsler 100 HFP 5100) under constant amplitude cyclic loading and ambient temperature. The stress ratio  $R$  is set to 0.1 and the frequencies are about 30 Hz. The fatigue crack growth rate curves were determined by experimental investigations and application of numerical simulations. The crack length  $a$  is detected by an optical measuring system. In conjunction with the recorded load cycles  $N$  the crack growth rates  $da/dN$  can be calculated. The equivalent stress intensity factors  $K_{eq}$  and the cyclic equivalent stress intensity factor  $\Delta K_{eq}$  are calculated according to Richard [3] as

$$K_{eq} = \frac{K_I}{2} + \frac{1}{2} \sqrt{K_I^2 + 4(\alpha_1 K_{II})^2 + 4(\alpha_2 K_{III})^2} \quad (1)$$

where  $\alpha_1 = K_{Ic}/K_{IIc}$  and  $\alpha_2 = K_{Ic}/K_{IIIc}$ .

There is no formula available to calculate the stress intensity factors for such anisotropic material. Hence, those are determined by the three-dimensional crack simulation program ADAPCRACK3D. The program uses the modified virtual crack closure method to determine the energy release rates and corresponding values of stress intensity factors [4]. The correlation function according to the ASTM standard E647-13 [2] to examine the crack length in order to the crack tip opening displacement is not applicable. Therefore, it is necessary to calculate the stress intensity factors corresponding to the determined crack lengths. A three-dimensional finite elements model of the specimen is constructed in the



commercial finite element program ABAQUS. The simulations are performed with ABAQUS and ADAPCRACK3D. Using the latter, the numerical simulations of the fatigue crack growth and the fracture mechanical analysis are computed. For crack propagation it is assumed that linear elastic fracture mechanics is valid [4].

For executing the numerical simulations Young's moduli are required. Those were needed, among other things, for calculating fracture mechanical parameters. Thus, values are chosen according to the determined ones (cf. Tab. 1). Consequently, due to reasonable simulation the inhomogeneous orthotropic material is approximated as a homogeneous orthotropic continuum.

Fibre direction	E1 [GPa]	E2 [GPa]	E3 [GPa]
0°	3	20	3
45°	3	4.2	4.2
90°	3	3	20

Table 1: Mechanical properties for numerical simulations.

The fatigue crack growth rate curve for specimens with fibre direction perpendicular to the loading direction is illustrated in Fig. 7. The  $da/dN$  versus  $\Delta K_{eq}$  data are plotted on logarithmic scales. The fatigue crack growth rate curves for other directions are shown in Figs. 8 (45°) and 9 (0°). For each curve a fit of the necessary Forman/Mettu equation parameters (Tab. 2) has been carried out. This crack growth equation [5] is given by

$$\frac{da}{dN} = C_{FM} \left[ \left( \frac{1-\gamma}{1-R} \right) \Delta K_{eq} \right]^n \frac{\left( 1 - \frac{\Delta K_{th}}{\Delta K_{eq}} \right)^p}{\left( 1 - \frac{K_{max}}{K_C} \right)^q} \tag{2}$$

Parameter	Fibre direction		
	0°	45°	90°
$C_{FM}$	5E-04	2E-04	9E-05
$\gamma$	0	0	0
$R$	0.1	0.1	0.1
$\Delta K_{th}$	0.8	0.9	1.0
$K_C$	4.5	9.0	9.0
$n$	3.5	2.0	2.5
$p$	5.0	3.0	2.5
$q$	0.50	0.25	0.25

Table 2: Forman/Mettu equation parameters.

It can be seen that near-threshold values can hardly be found due to the material and the sensitivity of the measurement system. Therefore, the threshold values can only be regarded as extrapolations. The data for the linear intervals are well-recorded, so that a fit of the parameters was possible. The slope of the fatigue crack growth rate curve for specimens with 0° fibre direction is much steeper than the other ones. The crack growth rate data for 45° specimens and 90° specimens are very similar.

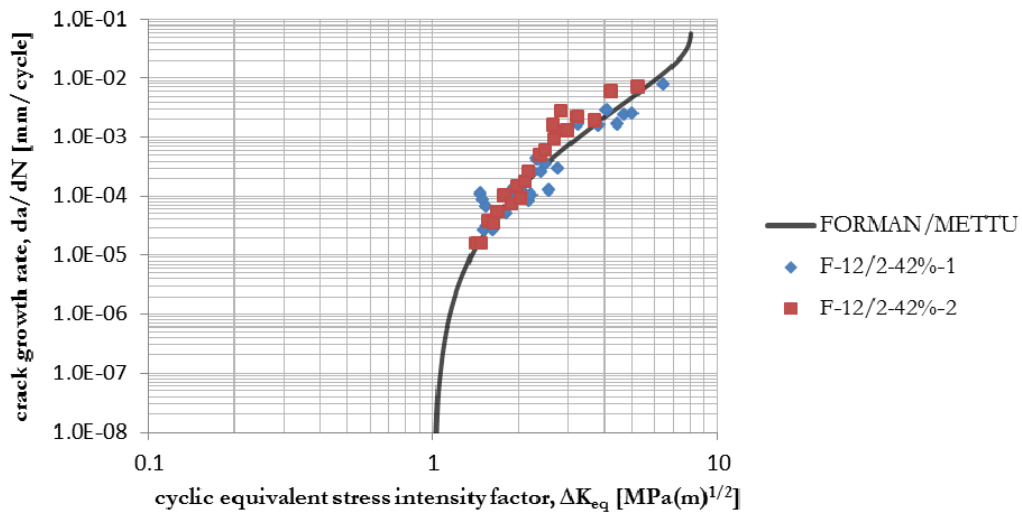


Figure 7: Fatigue crack growth rate data for compact tension specimens (90° fibre direction,  $R = 0.1$ ).

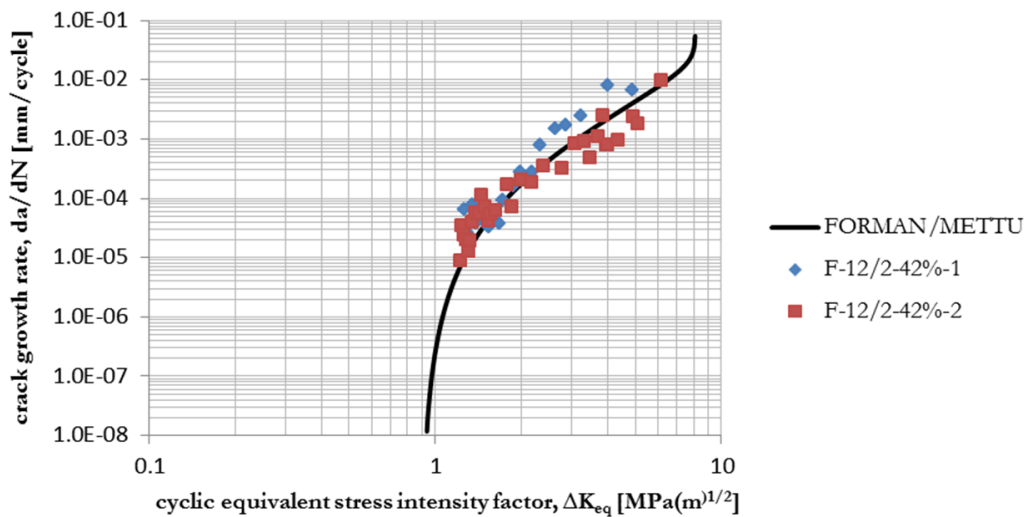


Figure 8: Fatigue crack growth rate data for compact tension specimens (45° fibre direction,  $R = 0.1$ ).

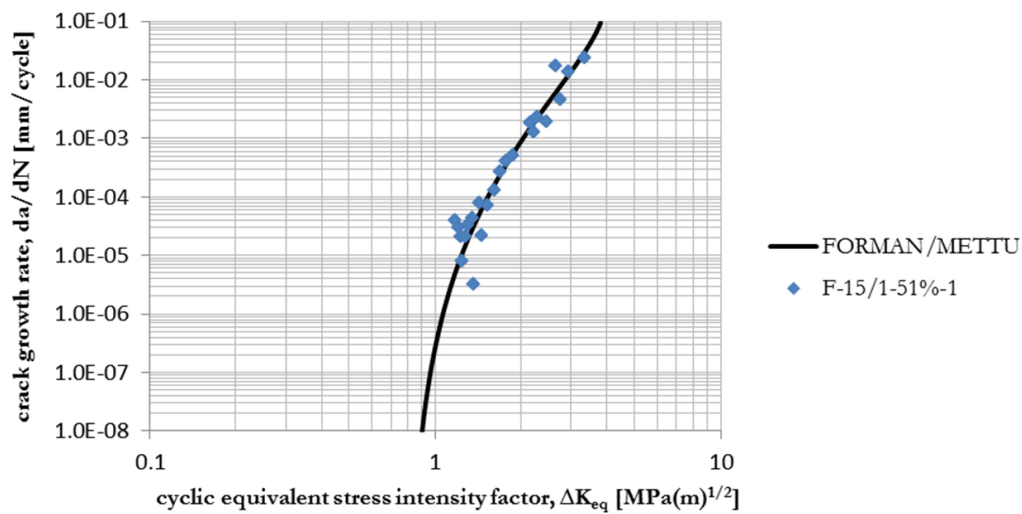


Figure 9: Fatigue crack growth rate data for compact tension specimen (0° fibre direction,  $R = 0.1$ ).



## GEOMETRY CORRECTION FACTOR FUNCTIONS

The evolution of the cyclic equivalent stress intensity factors with the growing crack does not follow the well-known stress intensity factor solution for compact tension specimens proposed by Srawley [6] since the material is no longer homogeneous and isotropic, in consequence the crack is not only governed by the stress state. It is necessary to carry out extensive numerical simulations to evaluate the stress intensity factor evolution along the growing crack in order to be able to determine fatigue crack growth rate curves. For numerical simulations experimentally determined crack lengths are required to calculate the corresponding stress intensity factors.

Hence, special functions for calculating the geometry correction factors for each fibre direction and fibre volume fraction are needed. Here, the geometry correction factor  $Y$  is computed with the equivalent stress intensity factor  $K_{eq}$ , the specimen thickness  $B$ , the length of the ligament (specimen width)  $X$ , and the applied force  $P$  to

$$Y = \frac{K_{eq} \cdot B \cdot \sqrt{X}}{P} \quad (3)$$

The single geometry correction factors can be expressed by a mathematical function. Commonly, the function depends on the crack length  $a$  and the length of the ligament, mostly named with the character  $W$ . Here, those lengths are denoted with the character  $X$  to point out that  $X$  is a directional parameter. For example, if the fibre direction is perpendicular to the loading direction ( $90^\circ$ ),  $X$  is assumed as the originally length of the ligament  $W$ . The function is described by

$$Y\left(\frac{a}{X}\right) = Y\left(\frac{a}{W}\right) = 5.5 + 2\left(\frac{a}{W}\right) + 20\left(\frac{a}{W}\right)^2 + 8\left(\frac{a}{W}\right)^3 + 70\left(\frac{a}{W}\right)^4 \quad (4)$$

By means of the geometry correction factor functions it is possible to calculate values of the stress intensity factor and obtain fatigue crack growth rate curves for different fibre directions. The geometry correction function data for a compact tension specimen with  $90^\circ$  fibre direction are plotted in Fig. 10. For further fibre directions functions need to be developed. Therefore, it is suitable to only modify the parameter  $X$  in Eq. (4). Concerning this matter the length of the ligament  $X$  could be changed directional.

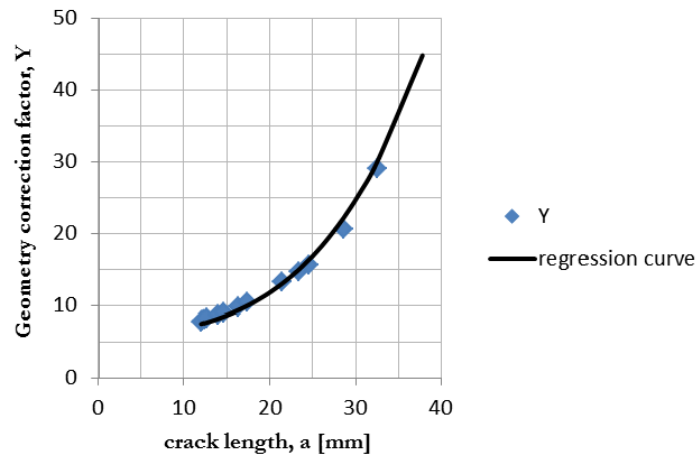


Figure 10: Geometry correction factor data for compact tension specimen ( $90^\circ$  fibre direction).

## CONCLUSIONS AND OUTLOOK

In this paper mechanical and fracture mechanical behaviour of natural fibre-reinforced composites were presented. Thereby, crack paths for compact tension specimens with different fibre directions and fibre volume fraction were under consideration. Both fibre direction and fibre volume fraction influence the crack path. The more fibres are



contained, the faster the crack path tends to grow in fibre direction. Here the ratio of the elasticity mismatch plays an important role. Also, as a first approach a formula for calculating the geometry correction factors for compact tension specimens where the fibre direction is perpendicular to the loading direction was described.

The geometry correction factor functions for further fibre directions need to be developed. Therefore, it is necessary to consider the possibility to only modify the parameter concerning the length of the ligament.

## ACKNOWLEDGEMENT

**T**his publication has been partially funded with support from the European Union, the European Social Fund (ESF) and the Free State of Saxony.

## REFERENCES

- [1] Dicker, M.P.M., Duckworth, P.F., Baker, A.A., Francois, G., Hazzard, M.K., Weaver, P.M., Green composites: A review of material attributes and complementary applications, *Composites: Part A: Applied Science and Manufacturing*, 56 (2014) 280–289.
- [2] ASTM Standard E647-13, Standard Test Method for Measurement of Fatigue Crack Growth Rates. American Society for Testing and Material, West Conshohocken, PA, (2013).
- [3] Richard, H.A., Fulland, M., Sander, M., Theoretical crack path prediction, *Fatigue & Fracture of Engineering Materials and Structures*, 28 (2015) 3–12.
- [4] Fulland, M., Steigemann, M., Richard, H.A., Specovius-Neugebauer, M., Development of stress intensities for cracks in FGMs with orientation perpendicular and parallel to the gradation, *Engineering Fracture Mechanics*, 95 (2012) 37–44.
- [5] Kuna, M., *Finite Elements in Fracture Mechanics. Theory-Numerics-Applications*, Springer, Heidelberg, (2013). DOI: 10.1007/978-94-007-6680-8.
- [6] Srawley, J.E., Wide range stress intensity factor expressions for ASTM E399 standard fracture toughness specimens, *International Journal of Fracture*, 12 (1976) 475.